Kyle H. Yeates
Department of Mechanical Engineering,
University of Washington,
Seattle, WA 98195;
Department of Veterans Affairs,
Center for Limb Loss and Mobility,
1660 S. Columbian Way MS-151,
Seattle, WA 98108
e-mail: kyle.yeates@gmail.com

Ava D. Segal
Department of Veterans Affairs,
Center for Limb Loss and Mobility,
1660 S. Columbian Way MS-151,
Seattle, WA 98108
e-mail: avasegal@gmail.com

Richard R. Neptune
Department of Mechanical Engineering,
The University of Texas at Austin,
Austin, TX 78712
e-mail: rneptune@mail.utexas.edu

Glenn K. Klute
Department of Mechanical Engineering,
University of Washington,
Seattle, WA 98195;
Department of Veterans Affairs,
Center for Limb Loss and Mobility,
1660 S. Columbian Way MS-151,
Seattle, WA 98108
e-mail: gklute@u.washington.edu

A Coronally Clutching Ankle to Improve Amputee Balance on Coronally Uneven and Unpredictable Terrain

To improve the balance of individuals with lower limb amputation on coronally uneven terrain, a coronally clutching ankle (CCA) was developed to actively adapt through ±15 deg of free coronal foot rotation during the first ~60 ms of initial contact. Three individuals with lower limb amputations were fit with the CCA and walked across an instrumented walkway with a middle step that was either flush, 15 deg inverted, or 15 deg everted. An opaque latex membrane was placed over the middle step, making the coronally uneven terrain unpredictable. Compared to participants' clinically prescribed prosthesis, the CCA exhibited significantly more coronal angular adaption during early stance. The CCA also improved participants' center of mass (COM) path regulation during the recovery step (reduced variation in mediolateral position) and reduced the use of the hip and stepping recovery strategies, suggesting it improved participants' balance and enabled a quicker recovery from the disturbance. However, use of the CCA did not significantly affect participants' ability to regulate their coronal angular momentum during the disturbance, suggesting that the CCA did not improve all elements of dynamic balance. Reducing the distance between the CCA's pivot axis and the base of the prosthetic foot might resolve this issue. These findings suggest that actively adapting the coronal plane angle of a prosthetic ankle can improve certain elements of balance for individuals with lower limb amputation who walk on coronally uneven and unpredictable terrain. [DOI: 10.1115/1.4040183]

1 Introduction

Many individuals with lower limb amputation have difficulty maintaining balance while walking, especially in real-world situations that require quick responses to changes in terrain. One quarter of outdoor falls, where a wide variety of uneven terrains exists, occur in the coronal plane [1]. Maintaining balance when stepping on uneven terrain can be particularly difficult for individuals with lower limb amputation, because they lack the foot-ankle muscles needed to compensate, resulting in decreased balance control [2–4].

Nonamputees are able to optimize the coronal plane properties of their ankle to maintain balance on coronally uneven and unpredictable terrain (Fig. 1) [5]. However, current prosthetic foot/ankle systems lack the ability to optimize their coronal plane properties dynamically, and instead rely on the static properties of split keels and/or elastomer bumper systems for adaption. Previous work suggests that such systems are insufficient for improving mediolateral balance, as shown by an increased stepping response after an error in ML foot placement [6]. Adaptive prosthetic technology, such as switched impedance and semi-active damping, may improve certain elements of amputee gait [7,8], but are currently only applied to the sagittal plane dynamics of prosthetic systems. Thus, potential benefits of coronally adaptive prostheses on gait and balance control remain unexplored.

Coronal plane balance is regulated by active muscle force generation, which affects three primary balance strategies: mediolateral foot placement, hip abduction/adduction, and ankle inversion/eversion [9]. These strategies help regulate the overall range of whole-body coronal angular momentum (RCAM) [2,10], which has been linked with the outcomes of clinical balance tests [11]. In addition to RCAM, the ability to regulate the whole-body center of mass (COM) trajectory also provides important information about balance control [12,13].

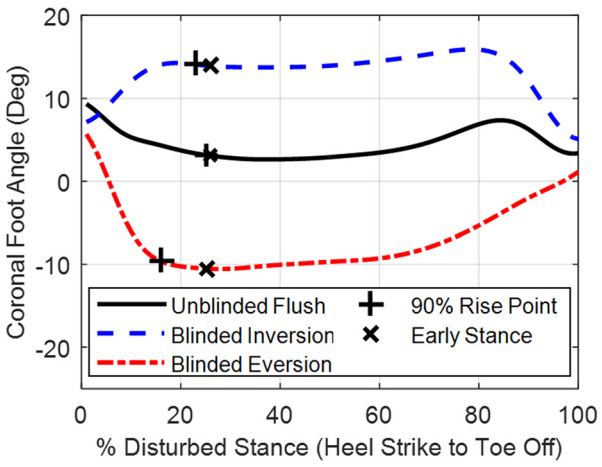

Fig. 1 Mean coronal foot angle with respect to the tibia of ten nonamputees walking on coronally uneven and unpredictable terrain [5]. Conditions shown for unblinded flush, blinded 15 deg inversion, and blinded 15 deg eversion terrain conditions. The point at which participants reached 90% of their maximum angular displacement for a given condition, and early stance, is shown for all conditions. Positive values associated with ankle inversion.

Manuscript received January 18, 2017; final manuscript received April 11, 2018; published online July 13, 2018. Assoc. Editor: Elizabeth Hsiao-Wecksler.

The purpose of this research was to improve the dynamic balance of individuals with lower limb amputation who walk on coronally uneven and unpredictable terrain. This paper describes the design, bench testing, and human subject experiments of a coronally clutching ankle (CCA) intended to conform to coronally uneven terrain. Measurement of participants' balance and recovery mechanisms demonstrated potential device efficacy and yielded information valuable to the development of future adaptive prostheses.

2 Methods

2.1 Device. Design of the CCA was based on nonamputee participants' ankle behavior during a step on coronally uneven terrain [5]. During the first 50% of the step, the coronal ankle angle reached 90% of its maximum deflection within an average of 162 ms after heel strike (HS) on uneven terrain (Fig. 1). At early stance, as defined by peak vertical ground reaction force (GRF, 182 ms mean for uneven terrain), the coronal ankle angle had an average difference from the flush condition of +11 deg for inversion and −13 deg for eversion (Fig. 1). After rapid adaption during early stance, ankle rotation appeared to be relatively slow, with the foot returning to a relatively neutral angle during toe-off. This suggested a prosthetic ankle that could angularly adapt during early stance would reduce the coronal ankle moment and thereby reduce the disturbance to balance.

Accordingly, the CCA was designed to adapt the coronal angle of a prosthetic foot to a similar degree and within a similar time as that of the human ankle during a step on coronally uneven terrain. The CCA axis of coronal rotation was immediately superior to the prosthetic foot's pyramid adapter (Fig. 2). This enabled angular conformation of the prosthetic foot to the terrain without large deformations of its internal split-keel, which may have generated substantial reactionary coronal moments. We hypothesized that compared to a standard prosthetic foot/ankle system, the CCA would decrease the coronal moment generated by stepping on to coronally uneven terrain, thereby improving balance of individuals with lower limb amputation.

The CCA (mass: 1.24 kg, build height: 165 mm) was mounted between a user's prosthetic socket and foot (Fig. 2) and used a clutch to enable or disable coronal rotation of the foot. The proximal section of the CCA was a rigid pylon structure, which housed the clutch and additional componentry that was not used for this study. The distal section was comprised of the prosthetic foot and foot-mount. The proximal and distal portions were hinged at the pivot shaft, and a Spectra rope (Honeywell, Morris Planes, NJ) (4.5 kN breaking strength) connecting the output spool of the clutch and the foot spool controlled their relative motion. A 1:5 ratio between the clutch and foot spools produced an angular stopping resolution at the foot-mount of 0.75 deg with 0.3 deg of backlash. Additionally, two restorative springs (average stiffness of 1.7 N/deg each) restored a neutral angle between the proximal and distal sections when the clutch was disengaged.

The clutch used a ratchet and pawl system to control rotation of the clutch spool, which was rigidly attached to the ratchet gear (Fig. 3). A set of eight pawls stopped rotation of the ratchet gear, which were biased with straight spring wire to engage the ratchet gear (Figs. 3 and 4). An upward motion of the pawl release arm disengaged the pawls and allowed rotation of the ratchet gear. A cam attached to a servo modified to rotate continuously (Model: S9650, Futaba, Mobara, Japan) drove this motion. From 0 deg to 180 deg of cam rotation, the pawl release arm was raised, enabling free spool rotation at approximately 160 deg. At 180 deg, a step in the cam, coupled with the bias of each of the pawl springs, rapidly lowered the position of the pawl release arm, allowing the pawls to engage the ratchet gear, and stopping the spool rotation.

The CCA operated untethered, was powered with a 7.4 V 1000 mAh lithium ion battery and was controlled with an Arduino Micro 3.3V (Arduino, Torino, Italy). Potentiometers (Model

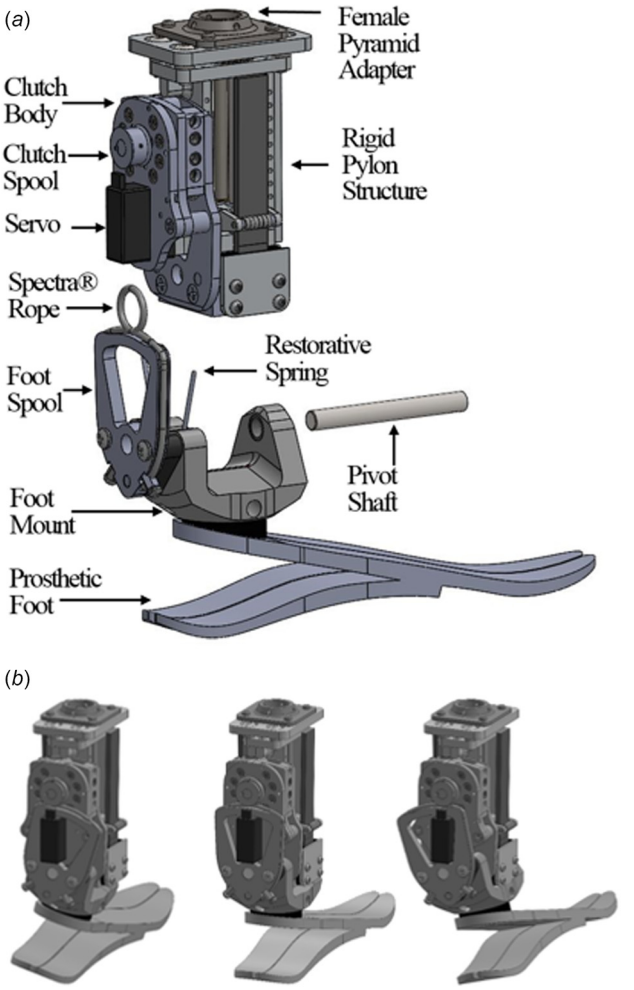

Fig. 2 (*a*) Expanded view of CCA with all major components grouped into the proximal section (top) and distal section (bottom). (*b*) Rear isometric views of CCA demonstrating the ±15 deg limit of foot-mount rotation. Note that only the foot-mount rotation was controlled by the CCA, and that elastic deformation within the prosthetic foot keel could create additional foot rotation.

SV01A103AEA01R00, Murata, Kyoto, Japan) measured servo, foot-mount, and spool angles; force sensitive resistors (model 402, Interlink, Camarillo, CA) measured plantar pressure; and a light sensor (Model ISL29125, Intersil, Milpitas, CA) detected a blue signal light that was strategically placed on the walkway to signal the CCA that the next step would be on uneven terrain (see Fig. 5). Other electronics included a micro-SD card for storing sensor measurements (recorded at 250Hz), an H-bridge motor driver (Model SN754410, Texas Instruments, Dallas, TX), and a simple user interface.

The controller was programmed specifically for the participant testing protocol and ensured the CCA only adapted when stepping on the disturbance, and returned the foot to a neutral angle and locked state prior to the recovery heel strike. Trials began with the CCA in a locked state. Prior to heel strike on the disturbance, the CCA would interpret presence of the signaling light and a lack of plantar pressure as a cue to enable free rotation of the clutch. At heel strike, the prosthetic foot would be free to adapt to the terrain for approximately 56 ms, which was the average time between the CCA sensing a spike in plantar pressure (indicating heel strike) and stopping clutch spool rotation. After toe-off from the disturbance, the CCA would free the clutch, which enabled the leaf springs to restore the foot to a neutral angle; and before the CCA's next heel strike, the clutch was again locked. The CCA

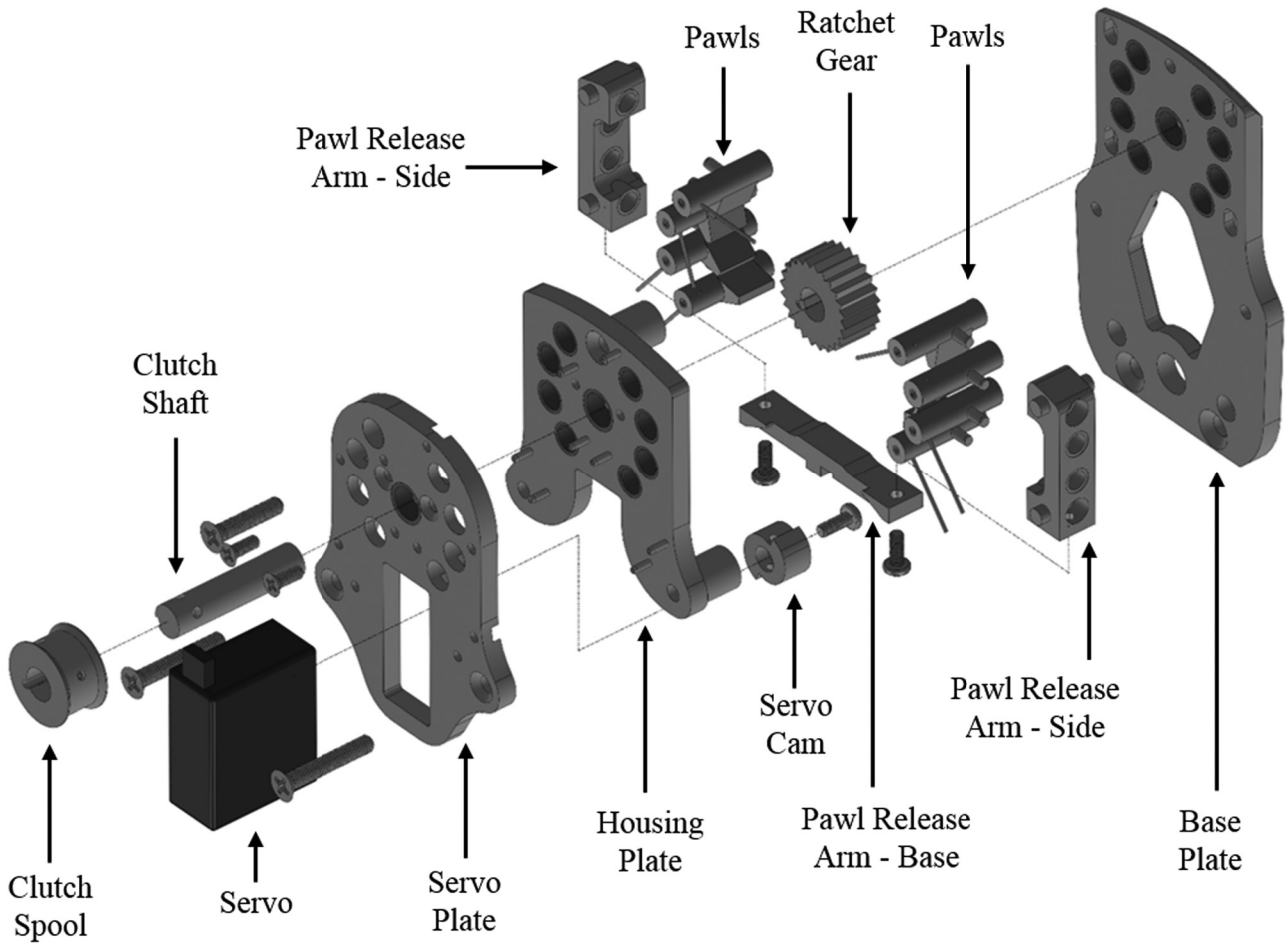

Fig. 3 Exploded view of the clutch in CCA device

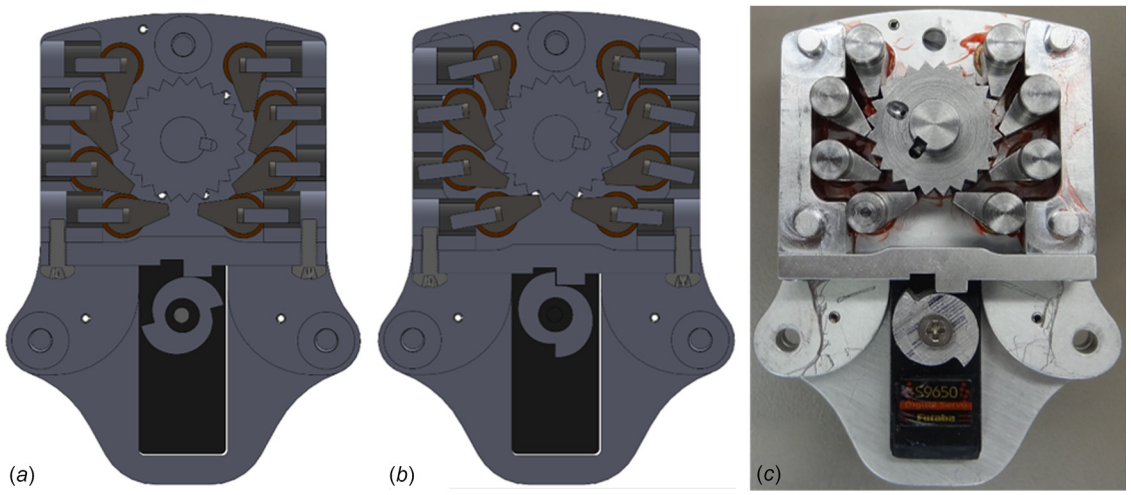

Fig. 4 (*a*) Cross section through the clutch in the free state showing how rotation of the servo cam translated the pawl release arm upward, disengaging the pawls and allowing the ratchet gear to spin freely, (*b*) cross section through the clutch in the locked state showing how rotation of the cam allowed the pawl release arm to move downward, allowing the spring-loaded pawls to engage the ratchet gear, ceasing its rotation, and (*c*) manufactured internal components of clutch

was designed to also operate in a locked mode. In the locked mode, rotation of the foot-mount relative to the pylon was physically disabled. However, both modes produced the same mechanical sounds to improve blinding of participants to the device condition.

2.2 Bench Tests and Results. Bench testing was carried out using a load frame testing system (model 858 Mini Bionix II, MTS, Eden Prairie, MN) and a custom base to simulate stepping on inverted and everted terrain [4]. The base consisted of a 15 deg coronally inclined surface which was mounted on a set of linear

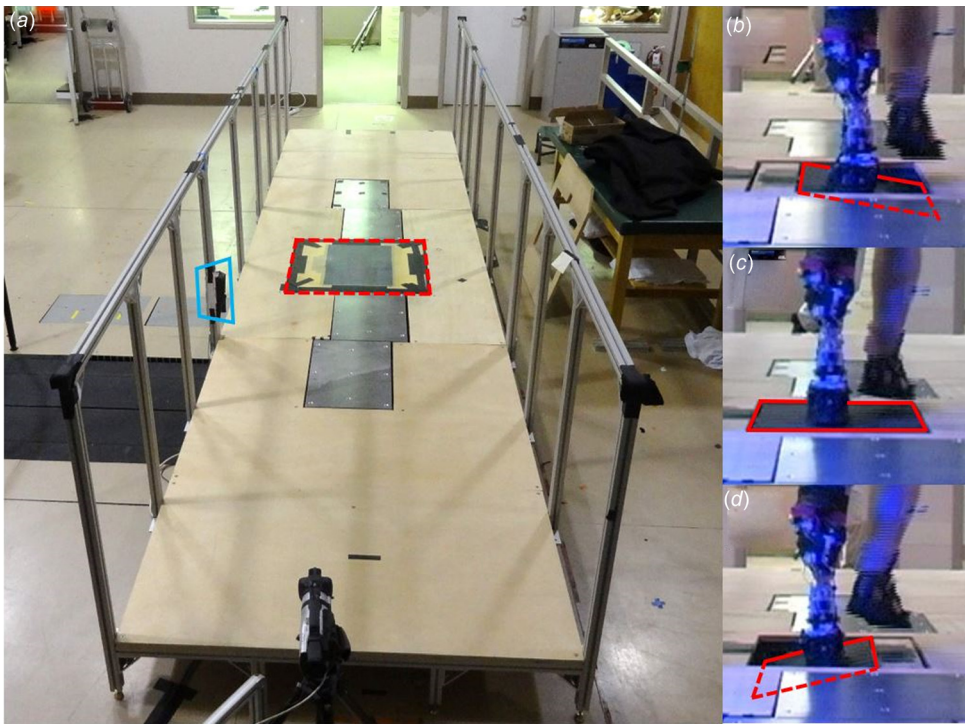

Fig. 5 (*a*) Walkway with embedded force plates, handrails, and signal light (blue trapezoid) for communication with CCA. The experimental setup is shown in the blinded condition, in which the disturbance device was concealed beneath a latex membrane (outlined by red dashed line). (*b*)–(*d*) Posterior view of a left amputee participant with CCA stepping on the disturbance device in the everted (*b*), flush (*c*), and inverted (*d*) positions. The experimental setup is shown without the latex membrane installed, and the portable force plate is highlighted with a red line.

bearings, allowing for mediolateral translation (Fig. 6). This prevented over-constraining the system and has been used in similar test procedures [14]. A Low Profile Vari-Flex foot (Ossur, Reykjavik, Iceland) with parameters representative of potential participants (size: 27, category: 4) was mounted to the CCA with a cosmetic shell and walking shoe (M577, New Balance, Boston, MA).

The test head was displaced at a rate of 50 mm/s with a load limit of 1000 N, which was sustained for a 1 s dwell period. The 1000 N load limit approximated the average maximum axial load through the tibia during control studies, while the loading rate was approximately 25% of that observed. The test was performed ten times each with an inverted, everted, and flat base. For all trials, the foot was initially positioned neutrally in all three rotational planes. Kinetic data from the bench tests were recorded at 120 Hz, and angular data from the CCA were recorded at 250 Hz.

Bench testing confirmed that the CCA was acceptable for human subject testing based on its response times and structural integrity (no plastic deformation observed). The CCA could cease rotation of the clutch spool with a 90% rise time (after heel strike) of 54–57 ms (Fig. 7(*a*)). At this point, rotation of the foot-mount slowed, but did not completely stop, as the foot-mount had a 90% rise time of 265–356 ms (Fig. 7(*b*)). Lag between the clutch spool and foot-mount rise times was attributed to stretch in the Spectra rope, which enabled approximately 3 deg of foot-mount rotation after the clutch spool ceased rotation (Fig. 7(*b*)). Due to the slow loading rate of the test, the additional 3 deg of rotation was a large portion of the overall range of motion of the foot-mount, and thus only when the Spectra rope was being stretched, could the foot-mount reach 90% of its overall range of motion. However, when the CCA stopped the clutch spool rotation, it appeared to have divided the foot-mount rotation into two modes: a preclutch mode characterized by relatively fast angular velocity of the foot-mount, and a post-clutch mode characterized by relatively slow angular velocity of the foot-mount (Fig. 7(*b*)). After the test load was

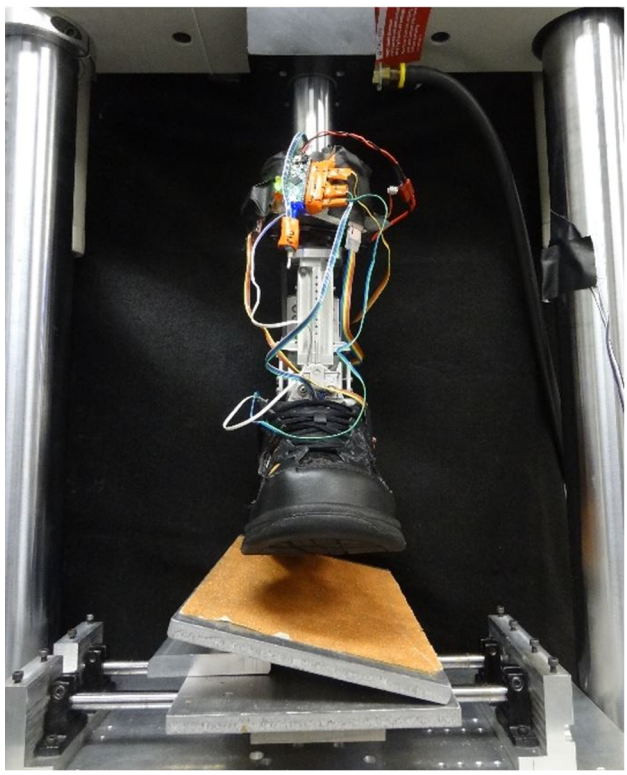

Fig. 6 Anterior view of bench testing for an inversion trial with a left foot. CCA with electronics shown mounted to the head of tester, with the sliding test base beneath.

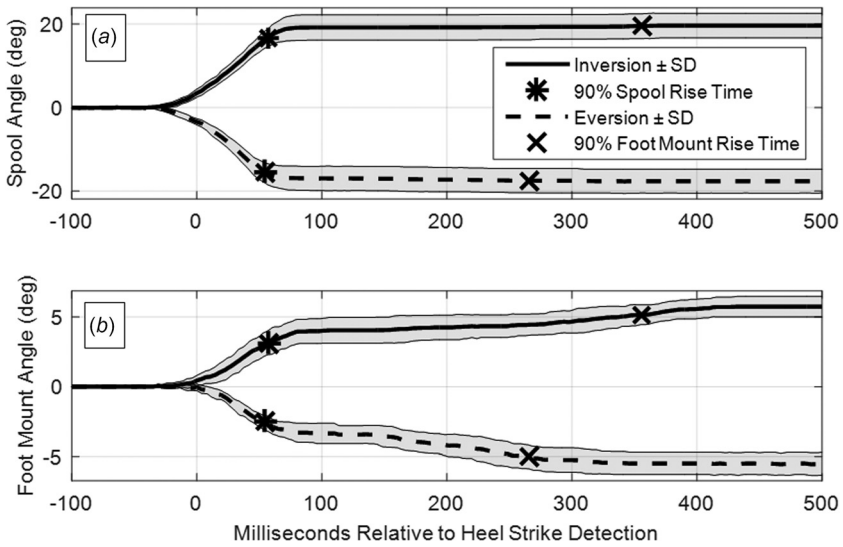

Fig. 7 Load frame test results for a 1000 N load with a feed rate of 50 mm/s. Time shown relative to HS detection. (*a*) Mean clutch spool angle in degrees for inversion and eversion. (*b*) Mean foot-mount angle in degrees for both inversion and eversion. ±SD symbolizes the corresponding data set's standard deviation is displayed in the figure.

released, it took an average of 428 ms for the CCA to neutralize the foot-mount angle and lock the clutch in preparation for the next heel strike. If the time between the disturbed heel off and the recovery heel strike of the prosthetic limb was shorter than needed by the CCA, the foot-mount could rotate ±15 deg in the coronal plane during the recovery step until the clutch locked. Based on the temporal data from the previous work [5], this scenario was considered unlikely; however, the stepping and hip strategies should also provide adequate recovery from such a scenario, with the handrails as an added precaution to avoid a fall.

2.3 Human Subject Experimental Setup. Coronally uneven and unpredictable terrain was produced in a gait lab using a walkway (8.0 m × 1.5 m) with a middle step onto a force plate (Model: 9286AA, Kistler, Winterthur, Switzerland) which could be rigidly positioned ±15 deg in the coronal plane, or flush with the walkway (Fig. 5). Researchers manually positioned the force plate in a custom jig and secured it with toggle-clamps and bolts [5]. The position of this disturbance could be concealed with a removable, opaque, latex membrane that was 0.5 mm thick. The isolated disturbance was intended to simulate stepping on a rock, object, or other singular coronal plane disturbance and allow for observation of balance recovery [5]. A LED was placed adjacent to the disturbance to signal its presence to the CCA (details in Sec. 2.1). The adjustable middle plate and four additional force plates (Model: BP400600, AMTI, Watertown, MS) allowed for kinetic data collection of the disturbed step, as well as the two steps before and after. A 12-camera motion capture system (Vicon Motion Systems, Oxford, UK) recorded marker trajectories at 120 Hz and force plate data at 1200 Hz. A digital, fourth order, low-pass Butterworth filter was applied with cutoff frequencies of 6 Hz for kinematic data and 25 Hz for kinetic data.

2.4 Human Subject Protocol. Participants donned a black spandex outfit, appropriately sized walking shoes (Model: M577, New Balance, Boston, MA), motion tracking markers, and either the CCA or their clinically prescribed (referred to as: as-prescribed) prosthesis. If the CCA was tested, a certified and licensed prosthetist aligned the CCA with the participant's existing socket and an appropriately sized and categorized low profile Vari-Flex foot. Anthropometric measures such as height, mass, limb length, joint width, and hallway self-selected walking speed were also recorded.

Testing occurred over two days. One day tested participant's as-prescribed prosthesis, while the other day tested the CCA device in the adapting and locked modes. The order of the as-prescribed prosthesis and CCA device testing days was randomized, as was the presentation of the CCA modes. While wearing each prosthesis, participants ambulated over inverted, everted, and flush terrain, as well as blinded inverted and blinded everted terrain. To familiarize participants with the terrain, unblinded trials were conducted prior to blinded trials. In the unblinded trials, terrain conditions were presented to the participants in a block randomized order with three to five repeated trials per position, depending on time constraints. For each condition, participants were instructed to walk at their self-selected speed across the walkway, and strike the disturbance device with their prosthetic foot. During blinded trials, the disturbance device was either inverted or everted, and the position was presented to participants in a random order, with three to five repeated trials per position, depending on time constraints. For all blinded trials, an opaque latex membrane was placed over the disturbance device to conceal its position to participants. Prior to each blinded trial, participants waited in a separate room behind a closed door to improve blinding of the terrain condition. The instructions given to participants were the same as those for the unblinded trials. Trials were rejected if participants' feet landed anywhere outside the force plates used to record the disturbed step, lead-in step, or recovery step. The disturbed step was completed with the prosthetic limb. The lead-in and recovery steps were completed with the intact limb, and occurred immediately before and after the disturbed step, respectively (Fig. 8).

2.5 Analysis. A 17-segment, modified Plug-In Gait model (Vicon Motion Systems Ltd, Oxford, UK) [15] was created in Visual 3D (C-Motion, Germantown, MD) and was used in combination with Matlab (Mathworks, Natick, MS) to produce the reported metrics [5]. To improve tracking of coronal plane foot motion, markers were placed on the first, second, and fifth metatarsal heads, and the insertion point of the Achille's tendon on the calcaneus, or the equivalent thereof on the prosthetic foot. For all prosthesis conditions, the residual limb and socket were modeled as a single rigid segment, and an ankle joint center (AJC) was

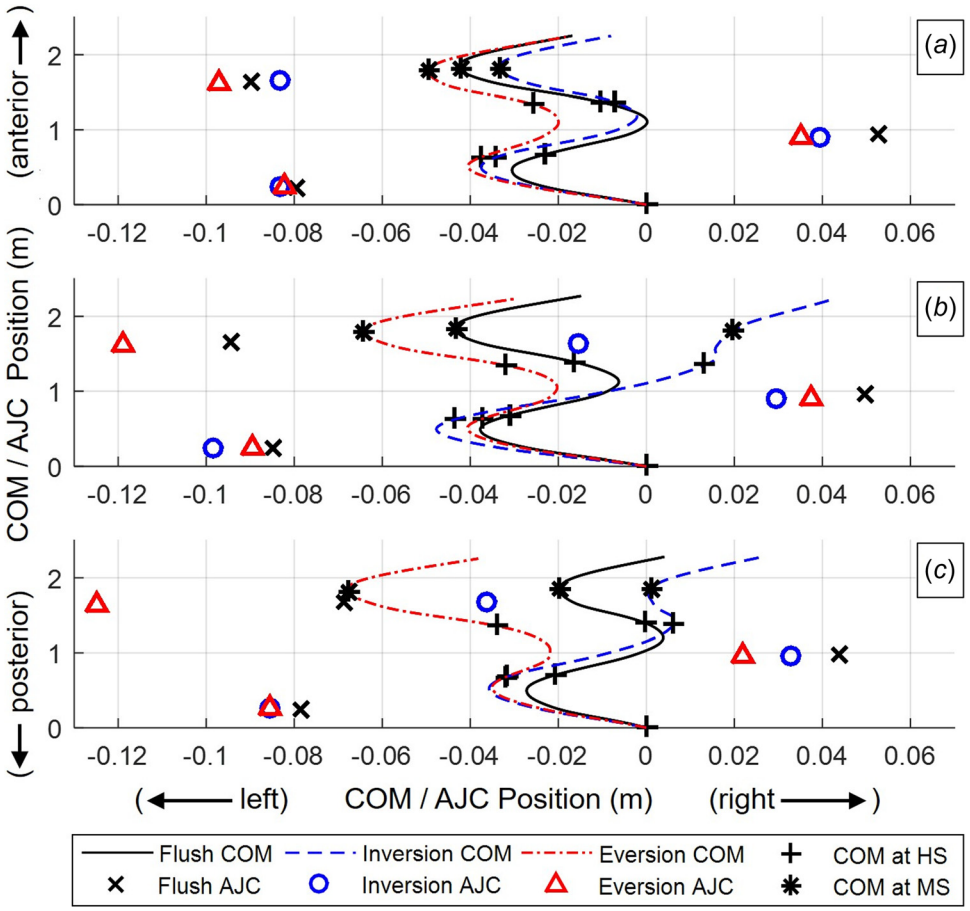

Fig. 8 Top down view of lab coordinate system displaying participants' mean COM path from intact limb lead-in step HS to intact limb recovery step toe off shown for (*a*) adapting CCA, (*b*) locked CCA, and (*c*) as-prescribed prosthesis conditions. COM location at HS of the three steps, as well as at midstance of the recovery step are marked. AJC location at HSs are also marked. All locations zeroed to lead-in step HS COM position, and left-amputee mediolateral data negated to match right-amputee participants.

defined as the midpoint between two markers that mirrored the medial and lateral malleoli of the intact limb. Additionally, the distal portion of the CCA was modeled as a separate segment from the prosthetic foot, allowing for independent tracking of the rigid foot-mount and flexible prosthetic foot relative to the proximal portion of the CCA. Inertial properties of the residual limb and socket remained constant between prosthesis conditions, while those for the CCA and as-prescribed prosthesis were adjusted to accommodate mass differences.

Adaption of the prosthetic foot and foot-mount were evaluated using Euler angles and were both calculated relative to the proximal segment of the CCA (or pylon for the as-prescribed prosthesis). The foot-mount angle measured rotation of the pyramid adapter of the prosthetic foot, which the CCA was designed to control. The foot angle measured the total rotation of the prosthetic foot, which encompassed the foot-mount angle and any additional elastic deformation of the foot keel. Both angles were measured at early stance, as defined by peak vertical GRF within the first 50% of stance. The 90% rise times were also calculated for the prosthetic foot angles and were used to evaluate the adaption speed of each prosthesis condition tested.

Regulation of the participant's COM trajectory during recovery was assessed using the mediolateral COM position at midstance of the recovery step relative to its position at heel strike of the lead-in step (recovery COM_X). Mediolateral foot position (MLFP) was used to evaluate the stepping strategy during recovery [5] and was defined as the mediolateral distance from the whole-body COM to the location of the AJC of the intact foot at heel strike on the recovery step. Heel strike was calculated as the first shoe contact with a force plate. The mediolateral impulse of the disturbed step was used to characterize external forces that may have affected elements of the participants' recovery, such as regulation of their COM trajectory and use of the stepping strategy. The mediolateral impulse was calculated by integrating the disturbed step mediolateral GRF (relative to the lab coordinate system) over the stance period of the disturbed step.

Gait balance during the disturbance was assessed using the RCAM between midstance of the lead-in step and midstance of the recovery step. This time period is referred to as the disturbed gait period, and the range was calculated as the difference between the highest and lowest values in that period [5]. Coronal moments about the CCA pivot axis (or for the as-prescribed prosthesis, an axis with the same orientation and location) and hip were characterized using their integral over the disturbed stance, a metric known as coronal angular impulse (CAI) [16].

Joint angles and moments of participants with a left lower limb amputation were negated to make all measures relative to those of participants with a right lower limb amputation. Recovery MLFP was normalized to body height. RCAM was normalized to walking speed, body height, and body mass. Joint moments and GRFs (and their corresponding integrals) were normalized to body mass.

2.6 Statistics. All statistical hypotheses were tested using a three-way, fixed-effects, analysis of variance (ANOVA) with an alpha level of 0.05. ANOVA factors were the prosthesis, terrain,

Table 1 *p*-Values resulting from three-way ANOVA testing of performance metrics. All metrics refer to disturbed stance or disturbed period unless otherwise noted. Pairwise comparisons performed between prosthesis conditions for a given terrain condition. Bolded *p*-values considered significant. Abbreviations: A, CCA Adapting; L, CCA locked; AP, as-prescribed; ES, early stance; CAI, coronal angular impulse; CCA, coronally clutching ankle; COM_X, center of mass mediolateral position; RCAM, range of coronal angular momentum; ML, mediolateral; MLFP, mediolateral foot position.

				Comparison between prostheses								
				Unblinded flush terrain			Blinded inversion terrain			Blinded eversion terrain		
Metric	Prosthesis main effect	Terrain main effect	Prosthesis-terrain interaction	A-L	L-AP	A-AP	A-L	L-AP	A-AP	A-L	L-AP	A-AP
ES foot angle	**0.001**	**<0.001**	**<0.001**	0.191	0.738	**0.002**	**<0.001**	0.391	**<0.001**	**<0.001**	**<0.001**	**<0.001**
CCA pivot CAI	**<0.001**	**<0.001**	**0.002**	0.998	0.068	**0.015**	**0.010**	0.149	0.986	**0.007**	**0.025**	1.000
Recovery COM_X	0.059	**<0.001**	**<0.001**	1.000	0.321	0.491	**<0.001**	0.638	**0.035**	0.876	1.000	0.737
Recovery MLFP	**0.038**	**<0.001**	**<0.001**	1.000	0.616	0.613	**<0.001**	0.674	**<0.001**	0.261	1.000	0.103
RCAM	**0.003**	**<0.001**	0.370	1.000	0.246	0.104	1.000	1.000	0.982	0.515	1.000	0.407
Hip CAI	0.254	**<0.001**	**<0.001**	0.998	0.999	1.000	**0.007**	**0.023**	1.000	0.082	1.000	0.168
ML impulse	0.694	**<0.001**	**0.012**	0.645	1.000	0.915	**0.047**	0.902	0.639	1.000	1.000	1.000

and participants, between each of which an interaction effect was included. Participants were used as an ANOVA factor, with each participant being treated as a unique category, due to the small sample size of the study (see Secs. 4.3 and 4.4 for further discussion). When appropriate, Tukey's honestly significant difference test was used to determine the significance of pairwise differences between prostheses within a given terrain condition. For RCAM, CAI about the CCA pivot, early stance foot angles, recovery MLFP, recovery COM_X, mediolateral (ML) impulse, and hip CAI, it was hypothesized that within a given uneven terrain condition, differences would exist between the prosthesis conditions.

3 Results

Three individuals with unilateral transtibial amputations of traumatic etiology provided informed consent to participate in this institutional review board approved study (mass: 86.2±3.6 kg, height: 1.80±0.03 m, age: 48.7±17.0 yr). All were male, had been fit with and used a prosthesis for over a year, ambulated without aids, and had no self-reported conditions that affected their gait. Participants' as-prescribed prosthetic feet were as follows: Vari-Flex, Vari-Flex XC, and Vari-Flex XC Rotate (Ossur, Reykjavik, Iceland). Each participant was able to complete at least three successful trials for each prosthesis/terrain condition combination.

The coronal early stance foot angle of participants exhibited significant prosthesis, terrain, and prosthesis–terrain interaction effects ($p \leq 0.001$) (Table 1). The early stance foot angle of the adapting CCA was significantly more inverted than other prosthesis conditions on inverted terrain ($p < 0.001$), and was significantly more everted than other prosthesis conditions on everted terrain ($p < 0.001$) (Fig. 9, Tables 1 and 2). Additionally, the foot angle of the adapting CCA at early stance on uneven terrain exhibited 15–17 deg of deviation from the flush condition, which was 6–10 deg more deviation when compared to the other prosthesis conditions (Fig. 9 and Table 2). When the CCA was adapting to uneven terrain, the coronal early stance angle of the foot-mount (Fig. 2) exhibited 9.1 deg and 2.5 deg less adaption than the prosthetic foot on inverted and everted terrain, respectively. The mean 90% rise time of the foot angle was 77 ms in inversion and was 142 ms in eversion for the adapting CCA (Table 2).

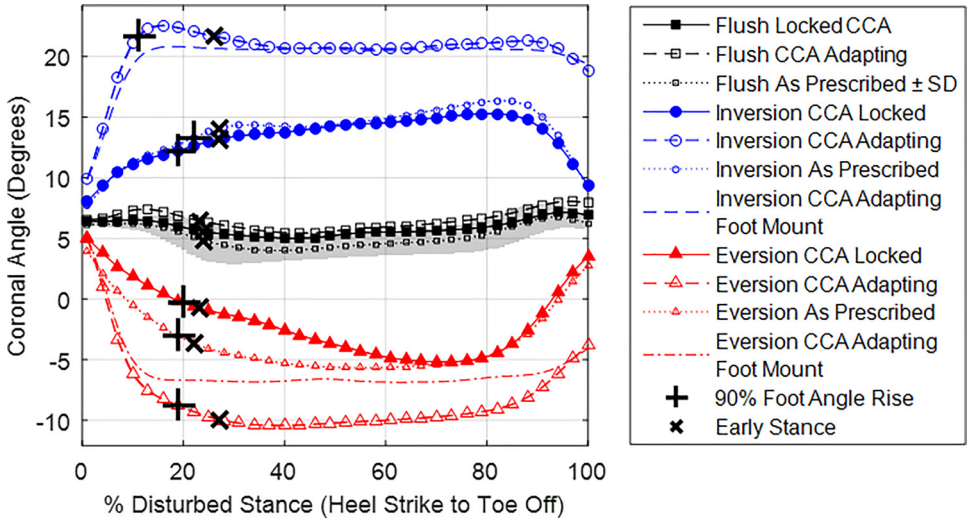

Fig. 9 Mean foot coronal angle with respect to the pylon (proximal portion of CCA) for all terrain and prosthesis combinations during the disturbed stance. For the CCA in adapting condition, position of the foot-mount with respect to the proximal portion of the CCA is also shown. A 90% rise time of foot angle on uneven terrain and an early stance for all conditions are shown for reference. Positive values associated with ankle inversion. ±SD symbolizes the corresponding data set's standard deviation is displayed in the figure.

Table 2 Mean and standard deviations (in parenthesis) for all performance metrics. All metrics refer to disturbed stance or disturbed period unless otherwise noted. Abbreviations: CCA, coronally clutching ankle; ES, early stance; RT, 90% rise time; CAI, coronal angular impulse; COM_X, center of mass mediolateral position in mid stance recovery step relative to its position at HS of the lead-in step; RCAM, range of coronal angular momentum; ML, mediolateral; MLFP, mediolateral foot position.

		Terrain and prosthesis conditions									
		Unblinded flush terrain			Blinded inversion terrain			Blinded eversion terrain			
Metric	Unit	CCA adapting	CCA locked	As-prescribed	CCA adapting	CCA locked	As-prescribed	CCA adapting	CCA locked	As-prescribed	
Complete trials	N/A	12	13	13	12	11	13	11	12	13	
ES foot angle	deg	6.6(2.3)	5.6(0.3)	4.9(0.3)	21.8(2.3)	13(1.4)	14.0(1.5)	−10.3(1.3)	−0.9(2.0)	−3.7(1.0)	
ES foot-mount ang.	deg	0.5(2.7)	−0.5(0.0)	N/A	12.7(3.8)	0.1(0.5)	N/A	−12.8(2.2)	−1.2(0.5)	N/A	
Foot angle RT	ms	115(30)	160(33)	135(35)	77(27)	131(28)	150(23)	142(50)	138(34)	134(32)	
CCA pivot CAI	N·m·s/kg	0.000(0.009)	0.004(0.010)	0.016(0.032)	−0.121(0.019)	−0.139(0.026)	−0.126(0.043)	0.134(0.014)	0.116(0.017)	0.131(0.048)	
Recovery COM_X	mm	−42(21)	−43(25)	−20(25)	−33(31)	20(37)	1(30)	−49(21)	−64(32)	−68(30)	
Recovery MLFP	mm	44(14)	43(10)	38(12)	42(15)	16(12)	24(14)	40(15)	48(16)	50(11)	
RCAM	N/A	0.043(0.009)	0.042(0.006)	0.038(0.006)	0.039(0.005)	0.038(0.007)	0.037(0.006)	0.054(0.009)	0.051(0.011)	0.051(0.007)	
Hip CAI	N·m·s/kg	−0.301(0.028)	−0.291(0.360)	−0.301(0.071)	−0.293(0.057)	−0.334(0.056)	−0.297(0.073)	−0.292(0.078)	−0.255(0.061)	−0.262(0.081)	
ML impulse	N·s/kg	−0.252(0.029)	−0.220(0.066)	−0.225(0.029)	−0.134(0.092)	−0.194(0.049)	−0.173(0.125)	−0.213(0.117)	−0.205(0.105)	−0.204(0.071)	

The CCA pivot CAI exhibited significant prosthesis, terrain, and prosthesis–terrain interaction effects ($p < 0.05$), as well as significant pairwise differences between prosthesis conditions within each of the terrain conditions (Table 1). However, the CCA pivot CAI appears tightly grouped by terrain condition (Fig. 10 and Table 1), with mean differences between terrain conditions being nearly an order of magnitude larger than mean differences between prosthesis conditions (Table 2).

The recovery COM_X exhibited a significant terrain effect ($p < 0.001$), and prosthesis–terrain interaction effect ($p < 0.001$) (Table 1). Recovery COM_X in blinded inversion was significantly ($p < 0.05$) different, positioned more toward the participants' left side (intact limb side) for the adapting CCA when compared to the other prosthesis conditions (Tables 1, 2, and Fig. 8). Additionally, across all terrain conditions, recovery COM_X for the adapting CCA appeared relatively constant (Fig. 8(*a*)); the mean recovery COM_X for the adapting CCA ranged from −33 to −49 mm (16 mm range), which was 19–23% of the magnitude of the ranges associated with the locked (84 mm) and as-prescribed (69 mm) conditions (Table 2).

The recovery MLFP exhibited significant prosthesis ($p = 0.038$), terrain ($p < 0.001$), and prosthesis–terrain interaction ($p < 0.001$) effects (Table 1). The adapting CCA condition in blinded inversion was significantly ($p < 0.001$) different (more lateral) when compared to other prosthesis conditions (Tables 1, 2, and Fig. 8). Additionally, across all terrain conditions, the mean recovery MLFP of the adapting CCA appeared relatively constant; ranging from 40 to 44 mm (4 mm range), which was 13–15% of the magnitude of the ranges associated with the locked (32 mm) and as-prescribed (26 mm) conditions (Table 2 and Fig. 8).

Range of coronal angular momentum was tightly grouped by terrain condition (Fig. 11 and Table 1). There were significant prosthesis ($p = 0.003$) and terrain ($p < 0.001$) main effects on RCAM; however, there were no significant pairwise differences between prosthesis conditions within a given terrain condition (Table 1). On average, RCAM in the blinded eversion condition was the largest, being 27–37% greater than that of the other terrain conditions (Table 2).

The hip CAI exhibited significant terrain, and prosthesis–terrain interaction effects ($p < 0.001$) (Table 1). Additionally, within the blinded inversion condition, significant differences ($p < 0.05$) were observed between the adapting and locked CCA conditions (Table 1). Closely related to the hip CAI, the hip moment during midstance appears to be tightly grouped by terrain condition, while differences between prosthesis conditions appear more pronounced during early stance (Fig. 12).

The disturbed step mediolateral impulse exhibited significant terrain and prosthesis–terrain interaction effects ($p < 0.05$) (Table 1). On average, the mediolateral impulse for inversion was more positive (laterally directed), and for eversion was more negative (medially directed). In blinded inversion, the mediolateral impulse for the adapting CCA condition was −0.134 N s/kg, which was significantly ($p = 0.047$) more positive (laterally directed) than that of the locked CCA condition (−0.194 N s/kg) (Table 2).

4 Discussion

4.1 Interpretation. The adapting CCA successfully conformed the coronal angle of the prosthetic foot to the uneven terrain, as indicated by significantly more inversion/eversion when compared to other prosthesis conditions (Fig. 9 and Table 1). The CCA foot-mount demonstrated a noticeably smaller range of motion (∼26 deg) than the prosthetic foot itself (∼32 deg) (Fig. 9 and Table 2), indicating the clutch stopped the foot-mount before it reached its maximum range of motion (30 deg), and that the last few degrees of the prosthetic foot's adaption were achieved through elastic deformation of the foot. The CCA did not exactly mimic the angular adaption of the biological foot (Fig. 1). Specifically, the adapting CCA had a 12–52% faster rise time and ∼25%

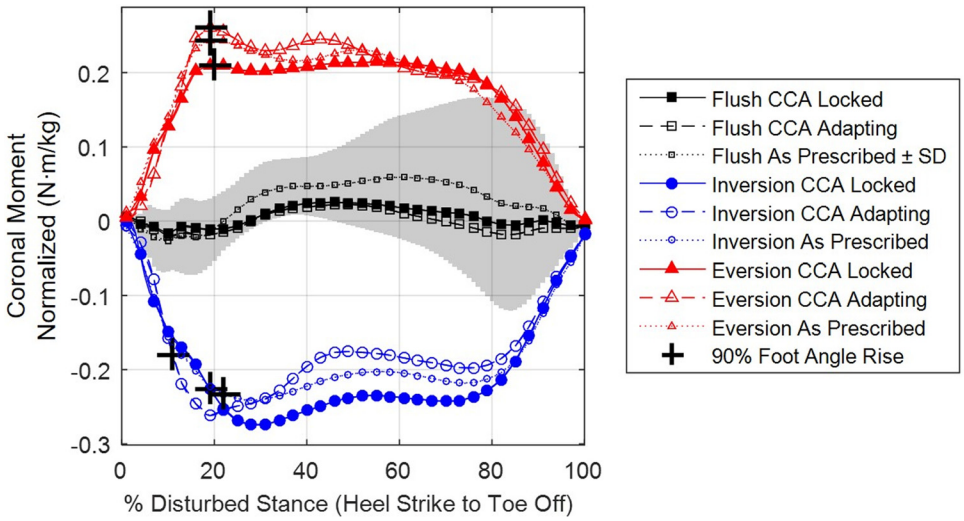

Fig. 10 Mean coronal moment about CCA pivot (or equivalent point for the as-prescribed prosthesis) over the disturbed stance for all prosthesis and terrain combinations. The 90% foot angle rise times for uneven terrain conditions are shown for reference. Positive values associated with ankle invertor moment. ±SD symbolizes the corresponding data set's standard deviation is displayed in the figure.

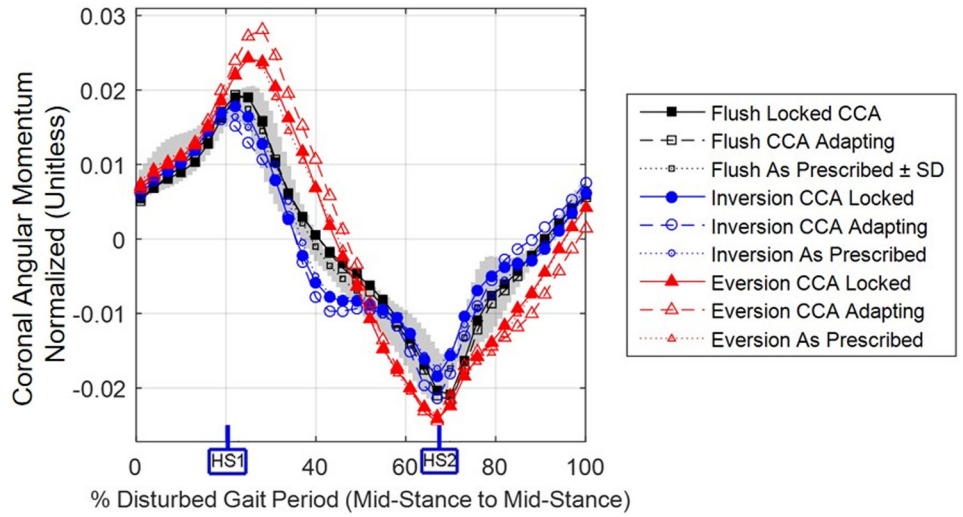

Fig. 11 Mean coronal angular momentum for all terrain and prosthesis combinations during the disturbed gait period. HS1 and HS2 signify HS of disturbed and recovery steps, respectively. Positive values associated with positive rotation about the participants' sagittal axis (originating from body and pointing anteriorly) [5]. ±SD symbolizes the corresponding data set's standard deviation is displayed in the figure.

larger range of motion in early stance (Table 2). Anecdotally, participants noticed the adapting mode of the CCA, describing it as "lively" and "active," suggesting that more nuanced adaptions might have been beneficial.

The adapting CCA was associated with improved regulation of the participants' COM path when walking on uneven terrain, as measured by the recovery COM_X. When equipped with the adapting CCA prosthesis, participants' recovery COM_X on uneven terrain was similar to the typical value of the participants' recovery COM_x during nondisturbed gait over flush terrain (Table 2). Additionally, when the adapting CCA prosthesis was used, the range of the participants' recovery COM_x over all terrain conditions was approximately 25% of the range associated with the other prosthesis conditions (Table 2). The improved COM path regulation associated with the adapting CCA is also visible in Fig. 8(*a*), in which the COM paths associated with inversion and eversion appear to deviate far less from the flush condition after stepping on uneven terrain conditions, when compared to the other prosthesis conditions (Figs. 8(*b*) and 8(*c*)).

Interestingly, adaption of the CCA did not appear to improve regulation of the participants' coronal angular momentum on uneven terrain, as indicated by the RCAM exhibiting no significant differences between prosthesis conditions for a given terrain (Table 1). In agreement with the previous work, amputee participants appeared less stable than nonamputees, as their RCAM was approximately 45% greater across all conditions [2,5]. We hypothesized that adaption of the CCA would improve the participants' ability to regulate coronal angular momentum by reducing the disturbance moment about the CCA pivot when stepping on uneven terrain. However, the CCA pivot CAI remained tightly grouped by terrain condition, and differences between prosthesis conditions were an order of magnitude smaller than the differences between terrain conditions (Fig. 10 and Table 2). Thus, it appears the prosthesis condition did not have a large enough effect

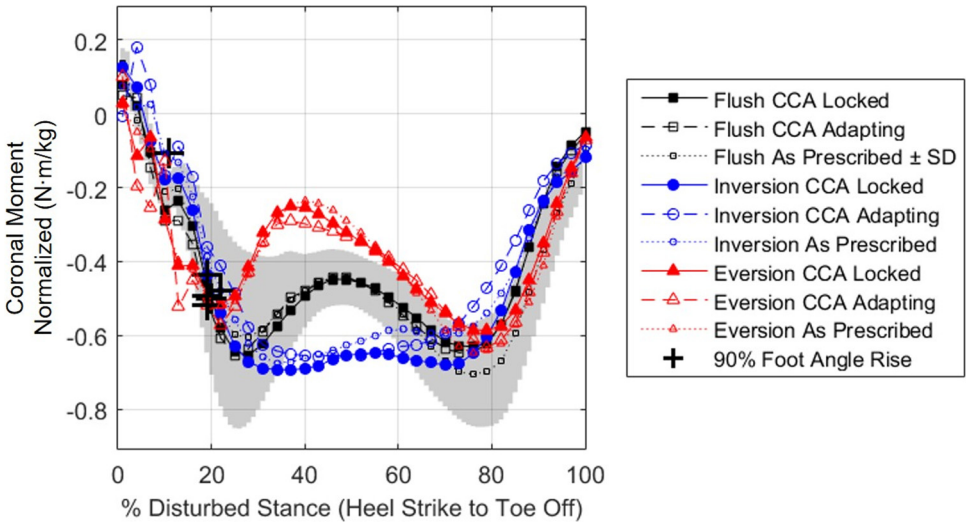

Fig. 12 Mean coronal hip moment over the disturbed stance for all prosthesis and terrain combinations. The 90% foot angle rise times for uneven terrain conditions are shown for reference. Positive values associated with hip adductor moment. ±SD symbolizes the corresponding data set's standard deviation is displayed in the figure.

on the CCA pivot moment to meaningfully affect participants' regulation of coronal angular momentum.

Adaption of the CCA had little effect on the moment about the CCA pivot due to the 120 mm length from the pivot to the base of support (bottom of the walking shoes, see Fig. 13). It appears that when the CCA was adapting to uneven terrain (Figs. 13(*a*) and 13(*b*)) the center of pressure translated relative to the base of support in a manner that would have reduced the moment arm of the GRF about the CCA pivot. However, at the same time, the base of support translated (by a distance proportional to the 120 mm length) in a manner that would have increased the moment arm of the GRF about the CCA pivot. Thus, when the CCA was adapting to uneven terrain the moment arm of the GRF about the pivot appears to have remained like that of the locked CCA (Figs. 13(*c*) and 13(*d*)). This seemingly constant moment arm likely explains the relatively constant CCA pivot moments observed across all prosthesis conditions within a given terrain (Fig. 10 and Table 2).

Coronally clutching ankle adaption was also associated with a reduction in the use of the hip and stepping strategies by participants as they recovered from the disturbance. The hip CAI during the disturbed stance exhibited a range of means between terrain conditions, which was 79–90% smaller than those associated with the other prosthesis conditions (Table 2). This suggests that the hip strategy was used less when the CCA was adapting. This was a departure from the response of nonamputees, who were shown to rely on the hip strategy during a step on uneven terrain and who also demonstrated larger coronal hip moment magnitudes across all terrain conditions [5]. In contrast, the stepping strategy used by participants with lower limb amputation when the CCA was adapting was more similar to the nonamputee response, when compared to the other prosthesis conditions. In both cases, minimal use of the stepping strategy was observed on the recovery step, as suggested by participants exhibiting a relatively small range of recovery MLFP across all terrain conditions (4–15 mm) [5], when compared to participants equipped with a nonadapting prosthesis (26–32 mm) (Table 2). These results, when coupled with a more regulated COM during the recovery step, suggest adaption of the CCA to uneven terrain enabled the participants to better regulate certain elements of their gait within the disturbed step, enabling a quicker recovery.

Further exploration of disturbed step kinetics revealed the mediolateral GRFs applied to the participants were significantly different when comparing the adapting CCA to other prosthesis conditions. Specifically, the adapting CCA was associated with a 20–30% more positive (more laterally directed) mediolateral ground reaction impulse when compared to the other prosthesis conditions in blinded inversion (Table 2). This difference was similar in magnitude to the mean difference between the terrain conditions, suggesting it likely had a substantial effect on the participants' recovery. Despite this more laterally directed impulse, the COM trajectory followed a similar path as unblinded flush and was positioned more to the left compared to the locked and as-prescribed conditions (Fig. 8). This unexpected response requires further exploration to relate differences in mediolateral impulse to the adaption of the CCA and the participants' ensuing recovery response.

4.2 Implications. We observed that adaption of the coronal angle of the prosthetic foot was associated with improved COM path regulation and reduced reliance on the stepping and hip strategy during recovery from uneven terrain. However, it should also be noted that without CCA adaption, the prosthetic foot still demonstrated approximately ±7 deg of coronal adaption through deformation. This range covers the maximum allowed grade of sidewalks as recommended by the U.S. Department of Transportation [17], and suggests that coronally adapting prostheses may provide the most benefit for amputees that ambulate in less controlled environments.

4.3 Limitations. A primary limitation was the small sample size ($n = 3$) used, and the use of a less conservative statistical model in which the subject effect was fixed. Thus, the results acquired could only be applied to the sample, and not the general population; however, these results support the potential efficacy of the CCA to improve balance and recovery from uneven terrain and rationalize further testing with a broader sample population. Another limitation was the short training period participants were given with the CCA. Had a more gradual training regime been implemented, participants may have become more familiar with the CCA, allowing them to better utilize its capabilities [18]. Finally, the terrain disturbance itself was limited in that all conditions were coupled with a slight step down, which was 7 mm for the flush condition, and 27 mm for the inverted and everted conditions.

4.4 Future Work. Future work will include conducting experiments with a larger sample population. Design revisions

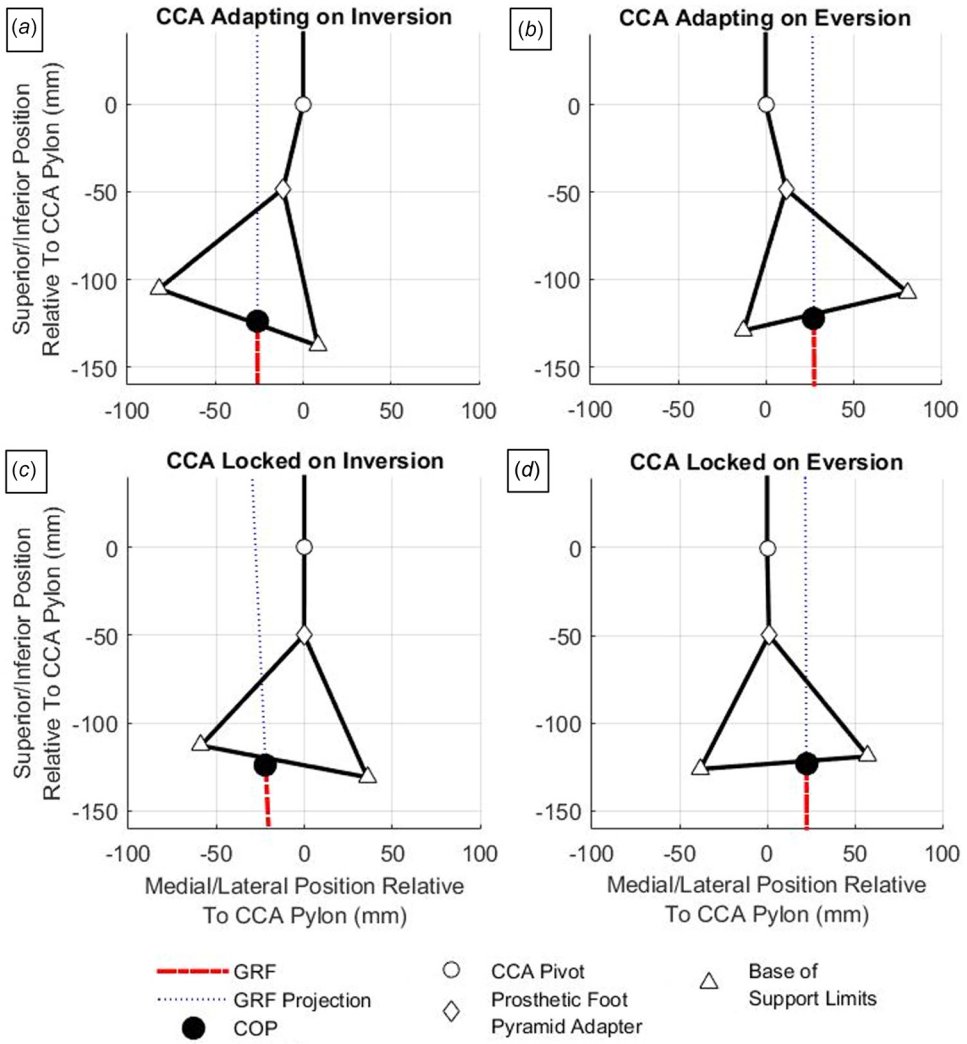

Fig. 13 Posterior view of the CCA, with the center of pressure and GRF during steps on inverted (*a*) and (*c*) and everted (*b*) and (*d*) terrain with the CCA in adapting (*a*) and (*b*) and locked (*c*) and (*d*) modes. All forces and locations are oriented relative to the proximal segment of the CCA. Images represent mean data from all participants at early stance. Data normalized to right side amputees, lateral and superior values are positive. Base of support limits are equivalent to the medial and lateral limits of the shoe.

may include reducing the distance between the CCA pivot and the base of support to enable the CCA to reduce the disturbance moment produced by coronally uneven terrain. Damping the rotation of the foot-mount may also be considered to allow the rise time of the prosthetic foot to be adjusted to better match that of the biological foot during a step on uneven terrain. Finally, future iterations of the CCA may use additional sensors to detect uneven terrain without the presence of a signal light.

Acknowledgment

Janice Pecoraro recruited participants, Krista Cyr assisted with data collection, and Daniel Daley, CPO, performed prosthesis fittings.

Funding Data

- This work was funded by the Department of Veterans Affairs, Rehabilitation Research and Development Service, Grants A9243C, RX001840, and A9248-S. The contents do not represent the views of the U.S. Department of Veterans Affairs or the United States Government.

References

[1] Li, W., Keegan, T. H. M., Sternfeld, B., Sidney, S., Quesenberry, C. P., and Kelsey, J. L., 2006, "Outdoor Falls Among Middle-Aged and Older Adults: A Neglected Public Health Problem," Am. J. Public Health, **96**(7), pp. 1192–1200.
[2] Silverman, A. K., and Neptune, R. R., 2011, "Differences in Whole-Body Angular Momentum Between Below-Knee Amputees and Non-Amputees Across Walking Speeds," J. Biomech., **44**(3), pp. 379–385.
[3] Neptune, R. R., and McGowan, C. P., 2011, "Muscle Contributions to Whole-Body Sagittal Plane Angular Momentum During Walking," J. Biomech., **44**(1), pp. 6–12.
[4] Neptune, R. R., and McGowan, C. P., 2016, "Muscle Contributions to Frontal Plane Angular Momentum During Walking," J. Biomech., **49**(13), pp. 2975–2981.
[5] Yeates, K. H., Segal, A. D., Neptune, R. R., and Klute, G. K., 2016, "Balance and Recovery on Coronally-Uneven and Unpredictable Terrain," J. Biomech., **49**(13), pp. 2734–2740.
[6] Segal, A., and Klute, G., 2014, "Lower-Limb Amputee Recovery Response to an Imposed Error in Mediolateral Foot Placement," J. Biomech., **47**(12), pp. 2911–2918.
[7] LaPre, A. K., and Sup, F., 2011, "Simulation of a Slope Adapting Ankle Prosthesis Provided by Semi-Active Damping," Annual International Conference of the IEEE Engineering in Medicine and Biology Society (EMBC), Boston, MA, Aug. 30–Sept. 3, pp. 587–590.
[8] Williams, R. J., Hansen, A. H., and Gard, S. A., 2009, "Prosthetic Ankle-Foot Mechanism Capable of Automatic Adaptation to the Walking Surface," ASME J. Biomech. Eng., **131**(3), p. 035002.
[9] MacKinnon, C. D., and Winter, D. A., 1993, "Control of Whole Body Balance in the Frontal Plane During Human Walking," J. Biomech., **26**(6), pp. 633–644.

[10] Herr, H., and Popovic, M., 2008, "Angular Momentum in Human Walking," J. Exp. Biol., **211**(4), pp. 467–481.
[11] Allum, J. H. J., Adkin, A. L., Carpenter, M. G., Held-Ziolkowska, M., Honegger, F., and Pierchala, K., 2001, "Trunk Sway Measures of Postural Stability During Clinical Balance Tests: Effects of a Unilateral Vestibular Deficit," Gait Posture, **14**(3), pp. 227–237.
[12] Hof, A. L., van Bockel, R. M., Schoppen, T., and Postema, K., 2007, "Control of Lateral Balance in Walking: Experimental Findings in Normal Subjects and above-Knee Amputees," Gait Posture, **25**(2), pp. 250–258.
[13] Marigold, D. S., and Patla, A. E., 2002, "Strategies for Dynamic Stability During Locomotion on a Slippery Surface: Effects of Prior Experience and Knowledge," J. Neurophysiol., **88**(1), pp. 339–353.
[14] Gorges, J. J., 2013, "Controlled Coronal Stiffness Prosthetic Ankle for Improving Balance on Uneven Terrain," Master's thesis, University of Washington, Seattle, WA.
[15] Ferrari, A., Benedetti, M. G., Pavan, E., Frigo, C., Bettinelli, D., Rabuffetti, M., Crenna, P., and Leardini, A., 2008, "Quantitative Comparison of Five Current Protocols in Gait Analysis," Gait Posture, **28**(2), pp. 207–216.
[16] Kobayashi, T., Orendurff, M. S., Arabian, A. K., Rosenbaum-Chou, T. G., and Boone, D. A., 2014, "Effect of Prosthetic Alignment Changes on Socket Reaction Moment Impulse During Walking in Transtibial Amputees," J. Biomech., **47**(6), pp. 1315–1323.
[17] Federal Highway Administration, 1999, "Chapter 4—Sidewalk Design Guidelines and Existing Practices," U.S. Department of Transportation, Washington, DC, accessed Feb. 9, 2016, http://www.fhwa.dot.gov/environment/bicycle_pedestrian/publications/sidewalks/chap4b.cfm
[18] Sawers, A., and Hahn, M. E., 2013, "Gradual Training Reduces Practice Difficulty While Preserving Motor Learning of a Novel Locomotor Task," Hum. Mov. Sci., **32**(4), pp. 605–617.